Trajectory Tracking Controls for Non-holonomic Systems Using Dynamic Feedback Linearization Based on Piecewise Multi-Linear Models

Tadanari Taniguchi and Michio Sugeno

Abstract—**This paper proposes a trajectory tracking control for non-holonomic systems using dynamic feedback linearization based on piecewise multi-linear (PML) models. The approximated model is fully parametric. Input-output (I/O) dynamic feedback linearization is applied to stabilize PML control system. Although the controller is simpler than the conventional I/O feedback linearization controller, the control performance based on PML model is the same as the conventional one. The proposed methods are applied to a tricycle robot and a quadrotor helicopter. Examples are shown to confirm the feasibility of our proposals by computer simulations.**

Index Terms—**piecewise model, tracking trajectory control, dynamic feedback linearization, non-holonomic system, tricycle robot and quadrotor helicopter.**

I. Introduction

Non-holonomic system has been intensively studied in control engineering by many researchers. But it is very difficult to control these systems because these systems cannot be asymptotically stabilized to an equilibrium point with smooth time-invariant state feedback control [1]. Therefore the non-holonomic system control is one of the challenging problems. In control engineering, a car robot dynamics, a linked robot arm model, hovercraft dynamics and helicopter dynamics are the typical non-holonomic systems.

This paper deals with a tracking trajectory control of a tricycle robot and a quadrotor helicopter using dynamic feedback linearization based on piecewise multi-linear (PML) models.

Wheeled mobile robots are completely controllable. However they cannot be stabilized to a desired position using time invariant continuous feedback control [2]. The wheeled mobile robot control systems have a non-holonomic constraint. Non-holonomic systems are much more difficult to control than holonomic ones. Many methods have been studied for the tracking control of wheeled robots. The experimental approaches were proposed in (e.g. [3], [4]). The backstepping control methods were proposed in (e.g. [5], [6]). The sliding mode control methods were proposed in (e.g., [7], [8]), and also the dynamic feedback linearization methods were in (e.g., [9], [10], [11]). For non-holonomic robots, it is never possible to achieve exact linearization via static state feedback [12]. It was shown that the dynamic feedback linearization is an efficient design tool to solve the trajectory tracking and the setpoint regulation problem in [9], [10].

First reported quadrotor helicopter *Gyroplane No.1* was built in 1907 by the Breguet Brothers [13]. A full-scale quadrotor helicopter was built by De Bothezat in 1921 [14]. Many methods have been applied to quadrotor helicopter control. A visual feedback based on feedback linearization and backstepping-like control were used in [15]. Dynamics feedback linearization method was applied by [16]. Sliding mode control methods were applied by [17], [18], [19], [13]. [17] and [19] designed the controller with the super twisting control algorithm based on sliding model control. [13] proposed a sliding mode controller to stabilize a cascaded underactuated system of helicopter. [20] applied a fuzzy controller and [21] proposed a reinforcement learning method to the quadrotor helicopter.

In this paper, we consider PML models as the piecewise approximation models of the tricycle robot and quadrotor dynamics. The models are built on hyper cubes partitioned in state space and are found to be bilinear (bi-affine) [22], so the models have simple nonlinearity. The model has the following features: 1) The PML model is derived from fuzzy if-then rules with singleton consequents. 2) It has a general approximation capability for nonlinear systems. 3) It is a piecewise nonlinear model and second simplest after the piecewise linear (PL) model. 4) It is continuous and fully parametric. The stabilizing conditions are represented by bilinear matrix inequalities (BMIs) [23], therefore, it takes long computing time to obtain a stabilizing controller. To overcome these difficulties, we have derived stabilizing conditions [24], [25], [26] based on feedback linearization, where [24] and [26] apply input-output linearization and [25] applies full-state linearization.

We propose a dynamic feedback linearization for PML control system and design the tracking controllers to a tricycle robot and a quadrotor. The control systems have the following features: 1) Only partial knowledge of vertices in piecewise regions is necessary, not overall knowledge of an objective plant. 2) These control systems are applicable to a wider class of nonlinear systems than conventional I/O linearization. 3) Although the controller is simpler than the conventional I/O feedback linearization controller, the tracking performance based on PML model is the same as the conventional one.

This paper is organized as follows. Section II introduces the canonical form of PML models. Section III presents dynamic feedback linearizations of the car-like robot and the quadrotor helicopter. Sections IV and V propose trajectory tracking controller designs using dynamic feedback lineariza-

Manuscript received August 2, 2017. This work was partially supported by the Grant-in-Aid for Scientific Research of Ministry of Education, Culture, Sports, Science and Technology, Japan (MEXT KAKENHI Grant Number 26330285).

T. Taniguchi is with IT Education Center, Tokai University, Hiratsuka, Kanagawa, 2591292 Japan e-mail: taniguchi@tokai-u.jp

M. Sugeno is with Tokyo Institute of Technology.

tion based on PML models of the tricycle robot and the quadrotor helicopter. Section VI shows examples demonstrating the feasibility of the proposed methods. Finally, section VII summarizes conclusions.

II. Canonical Forms of Piecewise Bilinear Models

A. Open-Loop Systems

In this section, we introduce PML models suggested in [22]. We deal with the two-dimensional case without loss of generality. Define vector $d(\sigma,\tau)$ and rectangle $R_{\sigma\tau}$ in two-dimensional space as $d(\sigma,\tau) \equiv (d_1(\sigma), d_2(\tau))^T$,

$$R_{\sigma\tau} \equiv [d_1(\sigma), d_1(\sigma+1)] \times [d_2(\tau), d_2(\tau+1)]. \tag{1}$$

σ and τ are integers: $-\infty < \sigma, \tau < \infty$ where $d_1(\sigma) < d_1(\sigma+1), d_2(\tau) < d_2(\tau+1)$ and $d(0,0) \equiv (d_1(0), d_2(0))^T$. Superscript ^{T} denotes a *transpose* operation.

For $x \in R_{\sigma\tau}$, the PML system is expressed as

$$\begin{cases} \dot{x} = \displaystyle\sum_{i=\sigma}^{\sigma+1}\sum_{j=\tau}^{\tau+1} \omega_1^i(x_1)\omega_2^j(x_2) f_o(i,j), \\ x = \displaystyle\sum_{i=\sigma}^{\sigma+1}\sum_{j=\tau}^{\tau+1} \omega_1^i(x_1)\omega_2^j(x_2) d(i,j), \end{cases} \tag{2}$$

where $f_o(i,j)$ is the vertex of nonlinear system $\dot{x} = f_o(x)$,

$$\begin{cases} \omega_1^\sigma(x_1) = (d_1(\sigma+1) - x_1)/(d_1(\sigma+1) - d_1(\sigma)), \\ \omega_1^{\sigma+1}(x_1) = (x_1 - d_1(\sigma))/(d_1(\sigma+1) - d_1(\sigma)), \\ \omega_2^\tau(x_2) = (d_2(\tau+1) - x_2)/(d_2(\tau+1) - d_2(\tau)), \\ \omega_2^{\tau+1}(x_2) = (x_2 - d_2(\tau))/(d_2(\tau+1) - d_2(\tau)), \end{cases} \tag{3}$$

and $\omega_1^i(x_1), \omega_2^j(x_2) \in [0,\ 1]$. In the above, we assume $f(0,0) = 0$ and $d(0,0) = 0$ to guarantee $\dot{x} = 0$ for $x = 0$.

A key point in the system is that state variable x is also expressed by a convex combination of $d(i,j)$ for $\omega_1^i(x_1)$ and $\omega_2^j(x_2)$, just as in the case of $\dot{x}$. As seen in equation (3), x is located inside $R_{\sigma\tau}$ which is a rectangle: a hypercube in general. That is, the expression of x is polytopic with four vertices $d(i,j)$. The model of $\dot{x} = f(x)$ is built on a rectangle including x in state space, it is also polytopic with four vertices $f(i,j)$. We call this form of the canonical model (2) parametric expression.

B. Closed-Loop Systems

We consider a two-dimensional nonlinear control system.

$$\begin{cases} \dot{x} = f_o(x) + g_o(x)u(x), \\ y = h_o(x). \end{cases} \tag{4}$$

The PML model (5) is constructed from a nonlinear system (4).

$$\begin{cases} \dot{x} = f(x) + g(x)u(x), \\ y = h(x), \end{cases} \tag{5}$$

where

$$\begin{cases} f(x) = \displaystyle\sum_{i=\sigma}^{\sigma+1}\sum_{j=\tau}^{\tau+1} \omega_1^i(x_1)\omega_2^j(x_2) f_o(i,j), \\ g(x) = \displaystyle\sum_{i=\sigma}^{\sigma+1}\sum_{j=\tau}^{\tau+1} \omega_1^i(x_1)\omega_2^j(x_2) g_o(i,j), \\ h(x) = \displaystyle\sum_{i=\sigma}^{\sigma+1}\sum_{j=\tau}^{\tau+1} \omega_1^i(x_1)\omega_2^j(x_2) h_o(i,j), \\ x = \displaystyle\sum_{i=\sigma}^{\sigma+1}\sum_{j=\tau}^{\tau+1} \omega_1^i(x_1)\omega_2^j(x_2) d(i,j), \end{cases} \tag{6}$$

and $f_o(i,j)$, $g_o(i,j)$, $h_o(i,j)$ and $d(i,j)$ are vertices of the nonlinear system (4). The modeling procedure in region $R_{\sigma\tau}$ is as follows:

1) Assign vertices $d(i,j)$ for $x_1 = d_1(\sigma)$, $d_1(\sigma+1)$, $x_2 = d_2(\tau)$, $d_2(\tau+1)$ of state vector x, then partition state space into piecewise regions (see Fig. 1).
2) Compute vertices $f_o(i,j)$, $g_o(i,j)$ and $h_o(i,j)$ in equation (6) by substituting values of $x_1 = d_1(\sigma)$, $d_1(\sigma+1)$ and $x_2 = d_2(\tau)$, $d_2(\tau+1)$ into original nonlinear functions $f_o(x)$, $g_o(x)$ and $h_o(x)$ in the system (4). Fig. 1 shows the expression of $f(x)$ and $x \in R_{\sigma\tau}$.

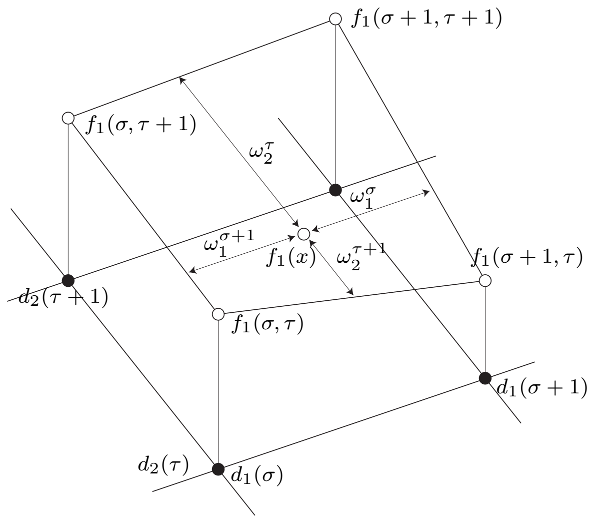

Fig. 1. Piecewise region ($f_1(x) = \sum_{i=\sigma}^{\sigma+1}\sum_{j=\tau}^{\tau+1} \omega_1^i\omega_2^j f_1(i,j)$, $x \in R_{\sigma\tau}$)

The overall PML model is obtained automatically when all vertices are assigned. Note that $f(x)$, $g(x)$ and $h(x)$ in the PML model coincide with those in the original system at vertices of all regions.

III. Dynamic Feedback Linearizations of Non-holonomic Systems

A. Tricycle Robot Model

We consider a tricycle robot model.

$$\begin{pmatrix} \dot{x} \\ \dot{y} \\ \dot{\theta} \\ \dot{\psi} \end{pmatrix} = \begin{pmatrix} \cos\theta \\ \sin\theta \\ \frac{1}{L}\tan\psi \\ 0 \end{pmatrix} u_1 + \begin{pmatrix} 0 \\ 0 \\ 0 \\ 1 \end{pmatrix} u_2, \tag{7}$$

where x and y are the position coordinates of the center of the rear wheel axis, θ is the angle between the center line of the car and the x axis, ψ is the steering angle with respect to the car. The control inputs are represented as

$$\begin{aligned} u_1 =& v_s \cos\psi \\ u_2 =& \dot{\psi}, \end{aligned}$$

where v_s is the driving speed. Fig 2 shows the kinematic model of tricycle robot. The steering angle ψ is constrained

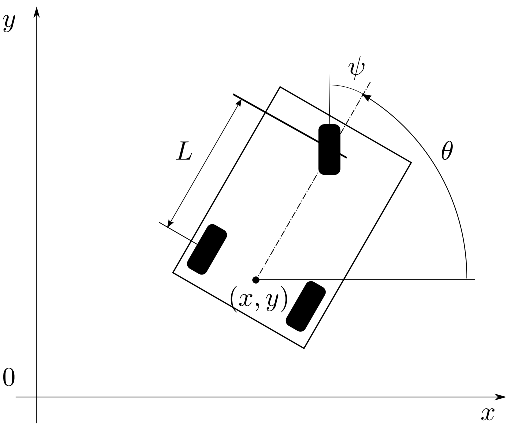

Fig. 2. Kinematic model of tricycle robot

by

$$\|\psi\| \le M, \ 0 < M < \pi/2.$$

The constraint [11] is represented as

$$\psi = M \tanh w,$$

where w is an auxiliary variable. Thus we get

$$\begin{aligned} \dot{\psi} =& M \mathrm{sech}^2 w \mu_2 = u_2, \\ \dot{w} =& \mu_2 \end{aligned}$$

We substitute the equations of ψ and w into the tricycle robot model. The model is obtained as

$$\begin{pmatrix} \dot{x} \\ \dot{y} \\ \dot{\theta} \\ \dot{w} \end{pmatrix} = \begin{pmatrix} \cos\theta \\ \sin\theta \\ \frac{1}{L}\tan(M\tanh w) \\ 0 \end{pmatrix} u_1 + \begin{pmatrix} 0 \\ 0 \\ 0 \\ 1 \end{pmatrix} \mu_2 \quad (8)$$

In this case, we consider $\eta = (x, y)^T$ as the output, the time derivative of η is calculated as

$$\dot{\eta} = \begin{pmatrix} \dot{x} \\ \dot{y} \end{pmatrix} = \begin{pmatrix} \cos\theta & 0 \\ \sin\theta & 0 \end{pmatrix} \begin{pmatrix} u_1 \\ \mu_2 \end{pmatrix}.$$

The linearized system of (8) at any points (x, y, θ, w) is clearly not controllable and the only u_1 affects $\dot{\eta}$. To proceed, we need to add some integrators of the input u_1. Using dynamic compensators as

$$\dot{u}_1 = \nu_1, \quad \dot{\nu}_1 = \mu_1,$$

the tricycle robot model (8) can be dynamic feedback linearizable. The extended model is obtained as

$$\begin{pmatrix} \dot{x} \\ \dot{y} \\ \dot{\theta} \\ \dot{w} \\ \dot{u}_1 \\ \dot{\nu}_1 \end{pmatrix} = \begin{pmatrix} u_1\cos\theta \\ u_1\sin\theta \\ u_1\frac{1}{L}\tan(M\tanh w) \\ 0 \\ \nu_1 \\ 0 \end{pmatrix} + \begin{pmatrix} 0 \\ 0 \\ 0 \\ 0 \\ 0 \\ 1 \end{pmatrix} \mu_1 + \begin{pmatrix} 0 \\ 0 \\ 0 \\ 1 \\ 0 \\ 0 \end{pmatrix} \mu_2 \quad (9)$$

The time derivative of $\dot{\eta}$ is calculated as

$$\ddot{\eta} = \begin{pmatrix} L_f^2 h_1 \\ L_f^2 h_2 \end{pmatrix} = \begin{pmatrix} \nu_1\cos\theta - u_1^2\frac{1}{L}\tan(M\tanh w)\sin\theta \\ \nu_1\sin\theta + u_1^2\frac{1}{L}\tan(M\tanh w)\cos\theta \end{pmatrix},$$

where $(h_1, h_2) = (x, y)$. Since the controller (μ_1, μ_2) doesn't appear in the equation $\dot{\eta}$, we continue to calculate the time derivative of $\ddot{\eta}$. Then we get

$$\begin{aligned} \eta^{(3)} =& L_f^3 h + L_g L_f^2 h \mu \\ =& \begin{pmatrix} L_f^3 h_1 \\ L_f^3 h_2 \end{pmatrix} + \begin{pmatrix} L_{g_1} L_f^2 h_1 & L_{g_2} L_f^2 h_1 \\ L_{g_1} L_f^2 h_2 & L_{g_2} L_f^2 h_2 \end{pmatrix} \begin{pmatrix} \mu_1 \\ \mu_2 \end{pmatrix}. \quad (10) \end{aligned}$$

Equation (10) shows clearly that the system is input-output linearizable because state feedback control

$$\mu = -(L_g L_f^2 h)^{-1} L_f^3 h + (L_g L_f^2 h)^{-1} v$$

reduces the input-output map to $y^{(3)} = v$.

The matrix $L_g L_f^2 h$ multiplying the modified input (μ_1, μ_2) is non-singular if $u_1 \neq 0$. Since the modified input is obtained as (μ_1, μ_2), the integrator with respect to the input v is added to the original input (u_1, u_2). Finally, the stabilizing controller of the tricycle robot system (7) is presented as a dynamic feedback controller:

$$\begin{cases} \dot{u}_1 = \nu_1, \ \dot{\nu}_1 = \mu_1, \\ u_2 = M \mathrm{sech}^2 w \mu_2 \end{cases} \quad (11)$$

B. Quadrotor Helicopter Model

We consider a quadrotor helicopter model [16].

$$\begin{cases} \dot{x} = f_o(x) + \sum_{i=1}^{4} g_{o_i}(x) u_{o_i} \\ y = h_o(x), \end{cases} \quad (12)$$

where $x = (x_0, \ y_0, \ z_0, \ \psi, \ \theta, \ \phi, \ v_1, \ v_2, \ v_3, p, \ q, \ r)^T$, $h_o(x) = (x_0, \ y_0, \ z_0, \ \psi)^T$, $u_o = (u_{o_1}, \ u_{o_2}, \ u_{o_3}, \ u_{o_4})^T$,

$$f_o(x) = \begin{pmatrix} v_1 \\ v_2 \\ v_3 \\ q\sin\phi\sec\theta + r\cos\phi\sec\theta \\ q\cos\phi - r\sin\phi \\ p + q\sin\theta\tan\theta + r\cos\phi\tan\theta \\ A_x/m \\ A_y/m \\ A_z/m + g \\ \frac{I_y - I_z}{I_x} qr + A_p/I_x \\ \frac{I_z - I_x}{I_y} rp + A_q/I_y \\ \frac{I_x - I_y}{I_z} pq + A_r/I_z \end{pmatrix}, \ g_{o_1} = \begin{pmatrix} 0 \\ 0 \\ 0 \\ 0 \\ 0 \\ 0 \\ G_1 \\ G_2 \\ G_3 \\ 0 \\ 0 \\ 0 \end{pmatrix},$$

$$\begin{aligned} G_1 =& -\frac{1}{m}(\cos\phi\cos\psi\sin\theta + \sin\phi\sin\psi), \\ G_2 =& -\frac{1}{m}(\cos\phi\sin\theta\sin\psi - \cos\psi\sin\theta), \\ G_3 =& -\frac{1}{m}\cos\theta\cos\phi, \end{aligned}$$

$$g_{o_2} = \begin{pmatrix} 0\\0\\0\\0\\0\\0\\0\\0\\0\\d/I_x\\0\\0 \end{pmatrix},\ g_{o_3} = \begin{pmatrix} 0\\0\\0\\0\\0\\0\\0\\0\\0\\0\\d/I_y\\0 \end{pmatrix},\ g_{o_4} = \begin{pmatrix} 0\\0\\0\\0\\0\\0\\0\\0\\0\\0\\0\\1/I_z \end{pmatrix}.$$

x_0, y_0 and z_0 are the three coordinates of the absolute

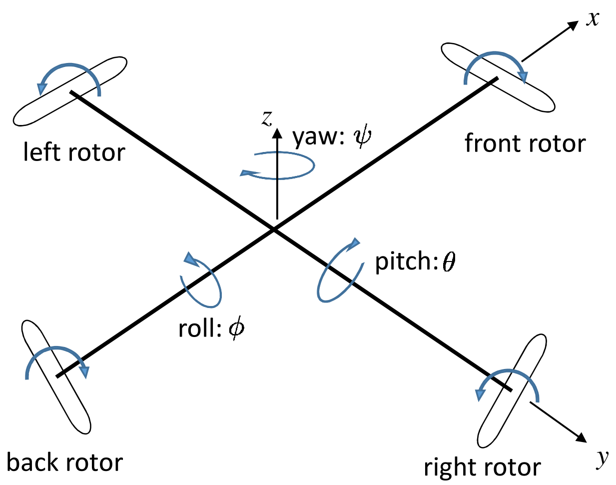

Fig. 3. Dynamic model of quadrotor

position of the quadrotor helicopter. ψ, θ and ϕ are the three Euler's angles of the attitude. These angles are yaw angle ($-\pi < \psi < \pi$), pitch angle ($-\pi/2 < \theta < \pi/2$) and roll angle ($-\pi/2 < \phi < \pi/2$) respectively. v_1, v_2 and v_3 are the absolute velocities of the quadrotor helicopter with respect to an earth fixed inertial reference frame. p, q and r are the angular velocities expressed with respect to a body reference frame. (A_x, A_y, A_z) and (A_p, A_q, A_r) are the resulting aerodynamics forces and moments acting on the quadrotor helicopter. I_x, I_y and I_z are the moment of inertia with respect to the axes. m is the mass, g is the gravity constant and d is the distance from the center of mass to the rotors. u_1 is the resulting thrust of the four rotors. u_2 is the difference of thrust between the left rotor and the right rotor. u_3 is the difference of thrust between the front rotor and the back rotor. u_4 is the difference of torque between the two clockwise turning rotors and the two counter-clockwise turning rotors.

We design a static state feedback controller [16] of the quadrotor helicopter model.

$$u_o = \alpha_o(x) + \beta_o(x)v_o \tag{13}$$

where $\alpha(x) = -A_o^{-1}(x)B_o(x)$, $\beta(x) = A_o^{-1}(x)$,

$$A_o(x) = \begin{pmatrix} G_1 & 0 & 0 & 0\\ G_2 & 0 & 0 & 0\\ G_3 & 0 & 0 & 0\\ 0 & 0 & d(\sin\phi\sec\theta)/I_y & \cos\phi\sec\theta/I_z \end{pmatrix},$$

$$B_o(x) = \left(L_{f_o}^2 h_{o_1}(x), L_{f_o}^2 h_{o_2}(x), L_{f_o}^2 h_{o_3}(x), L_{f_o}^2 h_{o_4}(x)\right)^T,$$

v_o is a controller of the linearized system with respect to (12). The linearized system of (12) for all x is clearly not controllable since $A_o(x)$ is singular. To proceed, we need to add some integrators of the input u_{o_1}.

Using dynamic compensators with respect to u_1 as

$$\zeta = u_{o_1},\ \xi = \dot{\zeta},\ \mu_{e_1} = \dot{\xi},$$

the quadrotor helicopter model (12) can be dynamic feedback linearizable. The other control inputs are also represented as

$$\mu_{e_2} = u_{o_2},\ \mu_{e_3} = u_{o_3},\ \mu_{e_4} = u_{o_4}.$$

Then the extended model is obtained as

$$\begin{cases} \dot{x} = f_e(x) + \sum_{i=1}^{4} g_{e_i}\mu_{e_i}, \\ y = h_o(x), \end{cases} \tag{14}$$

where $x = \left(x_0, y_0, z_0, \psi, \theta, \phi, v_1, v_2, v_3, p, q, r, \zeta, \xi\right)^T$,

$$f_e(x) = \begin{pmatrix} v_1\\ v_2\\ v_3\\ q\sin\phi\sec\theta + r\cos\phi\sec\theta\\ q\cos\phi - r\sin\phi\\ p + q\sin\theta\tan\theta + r\cos\phi\tan\theta\\ A_x/m + G_1\zeta\\ A_y/m + G_2\zeta\\ A_z/m + g + G_3\zeta\\ \frac{I_y - I_z}{I_x}qr + A_p/I_x\\ \frac{I_z - I_x}{I_y}rp + A_q/I_y\\ \frac{I_x - I_y}{I_z}pq + A_r/I_z\\ \xi\\ 0 \end{pmatrix},$$

$$\begin{aligned} g_{e_1} &= \left(0,\ 0,\ 0,\ 0,\ 0,\ 0,\ 0,\ 0,\ 0,\ 0,\ 0,\ 0,\ 0,\ 1\right)^T, \\ g_{e_2} &= \left(0,\ 0,\ 0,\ 0,\ 0,\ 0,\ 0,\ 0,\ 0,\ d/I_x,\ 0,\ 0,\ 0,\ 0\right)^T, \\ g_{e_3} &= \left(0,\ 0,\ 0,\ 0,\ 0,\ 0,\ 0,\ 0,\ 0,\ 0,\ d/I_y,\ 0,\ 0,\ 0\right)^T, \\ g_{e_4} &= \left(0,\ 0,\ 0,\ 0,\ 0,\ 0,\ 0,\ 0,\ 0,\ 0,\ 0,\ 1/I_z,\ 0,\ 0\right)^T. \end{aligned}$$

We apply the I/O feedback linearization to the extended system (14). Then the controller is obtained as

$$\mu_e = \alpha_e(x) + \beta_e(x)v_e$$

where $\alpha_e(x) = -A_e^{-1}(x)B_e(x)$, $\beta_e(x) = A_e^{-1}(x)$,

$$A_e(x) = \begin{pmatrix} a_{11} & a_{12} & a_{13} & 0\\ a_{21} & a_{22} & a_{23} & 0\\ a_{31} & a_{32} & a_{33} & 0\\ 0 & 0 & a_{43} & a_{44} \end{pmatrix},\ B_e(x) = \begin{pmatrix} L_{f_e}^4 h_{o_1}(x)\\ L_{f_e}^4 h_{o_2}(x)\\ L_{f_e}^4 h_{o_3}(x)\\ L_{f_e}^2 h_{o_4}(x) \end{pmatrix},$$

$$\begin{aligned} a_{ij} &= L_{g_{o_j}} L_{f_e}^3 h_{o_i}(x),\ i = 1,2,3,\ j = 1,2,3, \\ a_{4k} &= L_{g_{o_k}} L_{f_e} h_{o_4}(x),\ k = 3,4. \end{aligned}$$

The coordinate is obtained as

$$z_e = \left(z_{e_1},\ z_{e_2},\ z_{e_3},\ z_{e_4}\right)^T,$$

where

$$
\begin{aligned}
z_{e_1} &= \left(h_{o_1},\ L_{f_e}h_{o_1}(x),\ L_{f_e}^2 h_{o_1}(x),\ L_{f_e}^3 h_{o_1}(x)\right)^T,\\
z_{e_2} &= \left(h_{o_2},\ L_{f_e}h_{o_2}(x),\ L_{f_e}^2 h_{o_2}(x),\ L_{f_e}^3 h_{o_2}(x)\right)^T,\\
z_{e_3} &= \left(h_{o_3},\ L_{f_e}h_{o_3}(x),\ L_{f_e}^2 h_{o_3}(x),\ L_{f_e}^3 h_{o_3}(x)\right)^T,\\
z_{e_4} &= \left(h_{o_4}, L_{f_e}h_{o_4}(x)\right)^T.
\end{aligned}
$$

The I/O linearized system is formulated as

$$
\dot{z}_e = Az_e + Bv_e \tag{15}
$$

where

$$
A = \begin{pmatrix} A_1 & 0 & 0 & 0 \\ 0 & A_1 & 0 & 0 \\ 0 & 0 & A_1 & 0 \\ 0 & 0 & 0 & A_2 \end{pmatrix},\ B = \begin{pmatrix} B_1 & 0 & 0 & 0 \\ 0 & B_1 & 0 & 0 \\ 0 & 0 & B_1 & 0 \\ 0 & 0 & 0 & B_2 \end{pmatrix},
$$

$$
C = \begin{pmatrix} C_1 & 0 & 0 & 0 \\ 0 & C_1 & 0 & 0 \\ 0 & 0 & C_1 & 0 \\ 0 & 0 & 0 & C_2 \end{pmatrix},\ A_1 = \begin{pmatrix} 0 & 1 & 0 & 0 \\ 0 & 0 & 1 & 0 \\ 0 & 0 & 0 & 1 \\ 0 & 0 & 0 & 0 \end{pmatrix},
$$

$$
A_2 = \begin{pmatrix} 0 & 1 \\ 0 & 0 \end{pmatrix},\ B_1 = \begin{pmatrix} 0 & 0 & 0 & 1 \end{pmatrix}^T,\ B_2 = \begin{pmatrix} 0 & 1 \end{pmatrix}^T,
$$

$$
C_1 = \begin{pmatrix} 1 & 0 & 0 & 0 \end{pmatrix}, C_2 = \begin{pmatrix} 1 & 0 \end{pmatrix}.
$$

Stabilization linear controller $v_e = -Fz_e$ of the linearized system (15) is designed so that transfer function $C(sI - A)^{-1}B$ is Hurwitz.

IV. PML Model and Trajectory Tracking Controller Design of the Tricycle Robot Model

A. PML Model of the Tricycle Robot Model

We construct PML model [27] of the tricycle robot system (9). The state spaces of θ and w in the tricycle robot model (9) are divided by the 13 vertices $x_3 \in \{-\pi, -5\pi/6, \ldots, \pi\}$ and the 13 vertices $x_4 \in \{-3.0, -2.5, \ldots, 3.0\}$. The state variable is $x = (x_1, x_2, x_3, x_4, x_5, x_6)^T = (x, y, \theta, w, u_1, v_1)^T$.

$$
\dot{x} = \begin{pmatrix} \sum_{i_3=\sigma_3}^{\sigma_3+1} w_3^{i_3}(x_3) f_1(d_3(i_3))x_5 \\ \sum_{i_3=\sigma_3}^{\sigma_3+1} w_3^{i_3}(x_3) f_2(d_3(i_3))x_5 \\ \sum_{i_4=\sigma_4}^{\sigma_4+1} w_4^{i_4}(x_4) f_3(d_4(i_4))x_5 \\ 0 \\ x_6 \\ 0 \end{pmatrix} + \begin{pmatrix} 0 \\ 0 \\ 0 \\ 0 \\ 0 \\ 1 \end{pmatrix}\mu_1 + \begin{pmatrix} 0 \\ 0 \\ 0 \\ 1 \\ 0 \\ 0 \end{pmatrix}\mu_2. \tag{16}
$$

We can construct PML models with respect to $f_1(x)$, $f_2(x)$ and $f_3(x)$. The PML model structures are independent of the vertex positions x_5 and x_6 since x_5 and x_6 are the linear terms. This paper constructs the PML models with respect to the nonlinear terms of x_3 and x_4.

Note that trigonometric functions of the tricycle robot (9) are smooth functions and are of class C^∞. The PML models are not of class C^∞. In the tricycle robot control, we have to calculate the third derivatives of the output y. Therefore the derivative PML models lose some dynamics. In this paper we propose the derivative PML models of the trigonometric functions.

B. Stabilizing Control Using Dynamic Feedback Linearization Based on PML Model

We define the output as $\eta = (x_1, x_2)^T$ in the same manner as the previous section, the time derivative of η is calculated as

$$
\dot{\eta} = \begin{pmatrix} L_{f_p}h_1 \\ L_{f_p}h_2 \end{pmatrix} = \begin{pmatrix} \dot{x}_1 \\ \dot{x}_2 \end{pmatrix} = \sum_{i_3=\sigma_3}^{\sigma_3+1} w_3^{i_3}(x_3) \begin{pmatrix} f_1(d_3(i_3))x_5 \\ f_2(d_3(i_3))x_5 \end{pmatrix}
$$

where the vertices are $f_1(d_3(i_3)) = \cos d_3(i_3)$ and $f_2(d_3(i_3)) = \sin d_3(i_3)$. The time derivative of η doesn't contain the control inputs (μ_1, μ_2). We calculate the time derivative of $\dot{\eta}$. We get

$$
\begin{aligned}
\ddot{\eta}_1 =& L_{f_p}^2 h_1 = \sum_{i_3=\sigma_3}^{\sigma_3+1} w_3^{i_3}(x_3) f_1(d_3(i_3))x_6 \\
&+ \sum_{i_3=\sigma_3}^{\sigma_3+1} w_3^{i_3}(x_3) f_1'(d_3(i_3)) \sum_{i_4=\sigma_4}^{\sigma_4+1} w_4^{i_4}(x_4) f_3(d_4(i_4))x_5^2,\\
\ddot{\eta}_2 =& L_{f_p}^2 h_2 = \sum_{i_3=\sigma_3}^{\sigma_3+1} w_3^{i_3}(x_3) f_2(d_3(i_3))x_6 \\
&+ \sum_{i_3=\sigma_3}^{\sigma_3+1} w_3^{i_3}(x_3) f_2'(d_3(i_3)) \sum_{i_4=\sigma_4}^{\sigma_4+1} w_4^{i_4}(x_4) f_3(d_4(i_4))x_5^2,
\end{aligned}
$$

where $f_3(d_4(i_4)) = \tan(M \tanh d_4(i_4))/L$. We continue to calculate the time derivative of $\ddot{\eta}$. We get

$$
\begin{aligned}
\eta_1^{(3)} =& L_{f_p}^3 h_1 + L_{g_1} L_{f_p}^2 h_1 \mu_1 + L_{g_2} L_{f_p}^2 h_1 \mu_2 \\
=& x_5^3 \sum_{i_3=\sigma_3}^{\sigma_3+1} w_3^{i_3}(x_3) f_1^{''}(d_3(i_3)) \left(\sum_{i_4=\sigma_4}^{\sigma_4+1} w_4^{i_4}(x_4) f_3(d_4(i_4)) \right)^2 \\
&+ 3x_5x_6 \sum_{i_3=\sigma_3}^{\sigma_3+1} w_3^{i_3}(x_3) f_1^{'}(d_3(i_3)) \sum_{i_4=\sigma_4}^{\sigma_4+1} w_4^{i_4}(x_4) f_3(d_4(i_4)) \\
&+ \sum_{i_3=\sigma_3}^{\sigma_3+1} w_3^{i_3}(x_3) f_1(d_3(i_3))\mu_1 \\
&+ x_5^2 \sum_{i_3=\sigma_3}^{\sigma_3+1} w_3^{i_3}(x_3) f_1'(d_3(i_3)) \sum_{i_4=\sigma_4}^{\sigma_4+1} w_4^{i_4}(x_4) f_3'(d_4(i_4))\mu_2,
\end{aligned}
$$

$$
\begin{aligned}
\eta_2^{(3)} =& L_{f_p}^3 h_2 + L_{g_1} L_{f_p}^2 h_2 \mu_1 + L_{g_2} L_{f_p}^2 h_2 \mu_2 \\
=& x_5^3 \sum_{i_3=\sigma_3}^{\sigma_3+1} w_3^{i_3}(x_3) f_2^{''}(d_3(i_3)) \left(\sum_{i_4=\sigma_4}^{\sigma_4+1} w_4^{i_4}(x_4) f_3(d_4(i_4)) \right)^2 \\
&+ 3x_5x_6 \sum_{i_3=\sigma_3}^{\sigma_3+1} w_3^{i_3}(x_3) f_2^{'}(d_3(i_3)) \sum_{i_4=\sigma_4}^{\sigma_4+1} w_4^{i_4}(x_4) f_3(d_4(i_4)) \\
&+ \sum_{i_3=\sigma_3}^{\sigma_3+1} w_3^{i_3}(x_3) f_2(d_3(i_3))\mu_1 \\
&+ x_5^2 \sum_{i_3=\sigma_3}^{\sigma_3+1} w_3^{i_3}(x_3) f_2'(d_3(i_3)) \sum_{i_4=\sigma_4}^{\sigma_4+1} w_4^{i_4}(x_4) f_3'(d_4(i_4))\mu_2.
\end{aligned}
$$

The vertices $f_1^{''}(d_3(i_3))$, $f_2^{''}(d_3(i_3))$ and The controller of (16) is designed as

$$\begin{aligned}(\mu_1,\mu_2)^T =& -(L_gL_{f_p}^2h)^{-1}L_{f_p}^3h+(L_gL_{f_p}^2h)^{-1}v\\ =& -\begin{pmatrix}L_{g_1}L_{f_p}^2h_1 & L_{g_2}L_{f_p}^2h_1\\ L_{g_1}L_{f_p}^2h_2 & L_{g_2}L_{f_p}^2h_2\end{pmatrix}^{-1}\begin{pmatrix}L_{f_p}^3h_1\\ L_{f_p}^3h_2\end{pmatrix}\\ &+\begin{pmatrix}L_{g_1}L_{f_p}^2h_1 & L_{g_2}L_{f_p}^2h_1\\ L_{g_1}L_{f_p}^2h_2 & L_{g_2}L_{f_p}^2h_2\end{pmatrix}^{-1}v\end{aligned}$$

where v is the linear controller of the linear system (17).

$$\begin{cases}\dot{z} =Az+Bu,\\ y =Cz,\end{cases} \tag{17}$$

where $z=(h_1,\ L_{f_p}h_1,\ L_{f_p}^2h_1,\ h_2,\ L_{f_p}h_2,\ L_{f_p}^2h_2)^T\in\Re^6$,

$$A=\begin{pmatrix}0&1&0&0&0&0\\0&0&1&0&0&0\\0&0&0&0&0&0\\0&0&0&0&1&0\\0&0&0&0&0&1\\0&0&0&0&0&0\end{pmatrix}, B=\begin{pmatrix}0&0\\0&0\\1&0\\0&0\\0&0\\0&1\end{pmatrix}, C=\begin{pmatrix}1&0\\0&0\\0&0\\0&1\\0&0\\0&0\end{pmatrix}^T.$$

If $x_5\neq 0$, there exists a controller $(\mu_1,\mu_2)^T$ of the tricycle robot model (16) since $\det(L_gL_{f_p}^2h)\neq 0$.

In this case, the state space of the tricycle robot model is divided into 13×13 vertices. Therefore the system has 12×12 local PML models. Note that all the linearized systems of these PML models are the same as the linear system (17).

In the same manner of (11), the dynamic feedback linearizing controller of the PML system is designed as

$$\begin{cases}\ddot{u}_1 =\mu_1,\\ u_2 =M\mathrm{sech}^2x_4\mu_2,\\ \begin{pmatrix}\mu_1\\ \mu_2\end{pmatrix} =L_{f_p}^3h+L_gL_f^2hv.\end{cases} \tag{18}$$

The stabilizing linear controller $v=-Fz$ of the linearized system (17) is designed so that the transfer function $C(sI-A)^{-1}B$ is Hurwitz.

Note that the dynamic controller (18) based on PML model is simpler than the conventional one (11). Since the nonlinear terms of controller (18) contain not the original nonlinear terms (e.g., $\sin x_3$, $\cos x_3$, $\tan(M\tanh x_4)$) but the piecewise approximation models.

C. Trajectory Tracking Controller Based on PML System

We propose a tracking control [28] to the tricycle robot model (7). Consider the following reference signal model

$$\begin{cases}\dot{x}_r =f_r,\\ \eta_r =h_r.\end{cases}$$

The controller is designed to make the error signal $e=(e_1,e_2)^T=\eta-\eta_r\to 0$ as $t\to\infty$. The time derivative of e is obtained as

$$\dot{e} =\dot{\eta}-\dot{\eta}_r=\begin{pmatrix}L_{f_p}h_{p1}\\ L_{f_p}h_{p2}\end{pmatrix}-\begin{pmatrix}L_{f_r}h_{r1}\\ L_{f_r}h_{r2}\end{pmatrix}.$$

Furthermore the time derivative of $\dot{e}$ is calculated as

$$\ddot{e} =\ddot{\eta}-\ddot{\eta}_r=\begin{pmatrix}L_{f_p}^2h_{p1}\\ L_{f_p}^2h_{p2}\end{pmatrix}-\begin{pmatrix}L_{f_r}^2h_{r1}\\ L_{f_r}^2h_{r2}\end{pmatrix}$$

Since the controller μ doesn't appear in the equation $\ddot{e}$, we calculate the time derivative of $\ddot{e}$.

$$\begin{aligned}e^{(3)} =&\eta^{(3)}-\eta_r^{(3)}\\ =&\begin{pmatrix}L_{f_p}^3h_{p1}\\ L_{f_p}^3h_{p2}\end{pmatrix}+L_gL_{f_p}^2h\begin{pmatrix}\mu_1\\ \mu_2\end{pmatrix}-\begin{pmatrix}L_{f_r}^3h_{r1}\\ L_{f_r}^3h_{r2}\end{pmatrix}\end{aligned}$$

The tracking controller is designed as

$$\begin{cases}\ddot{u}_1 =\mu_1,\\ u_2 =M\mathrm{sech}^2x_4\mu_2,\\ \begin{pmatrix}\mu_1\\ \mu_2\end{pmatrix} =L_{f_p}^3h-L_{f_r}^3h_r+L_gL_{f_p}^2hv.\end{cases} \tag{19}$$

The linearized system (17) and controller $v=-Fz$ are obtained in the same manners as the previous subsection. The coordinate transformation vector is $z=(e_1,\ \dot{e}_1,\ \ddot{e}_1, e_2,\ \dot{e}_2,\ \ddot{e}_2)^T$.

Note that the dynamic controller (19) based on PML model is simpler than the conventional one on the same reason of the previous subsection.

V. PML Model and Trajectory Tracking Controller Design of the Quadrotor Helicopter

A. PML Model of the Quadrotor Helicopter

We construct PML model [29] of the quadrotor helicopter system (14). The state spaces of ψ, θ and ϕ in the quadrotor helicopter model (14) are divided by the following vertices.

$$\begin{aligned}x_4 =&\psi\in\{-\pi,-5\pi/6,-2\pi/3,\dots,\pi\},\\ x_5 =&\theta\in\{-5\pi/12,-\delta_1,-\delta_1/2,0,\delta_1/2,\delta_1,5\pi/12\},\\ x_6 =&\phi\in\{-5\pi/12,-\delta_2,-\delta_2/2,0,\delta_2/2,\delta_2,5\pi/12\}.\end{aligned}$$

where $\delta_1=\delta_2=\pi/200$. We construct the following PML model of the quadrotor helicopter model (14).

$$\begin{cases}\dot{x} =f(x)+\sum_{i=1}^{4}g_i\mu_i,\\ y =h(x)\end{cases} \tag{20}$$

where

$$\begin{aligned}f(x) =&\left(x_7,x_8,x_9,f_4,f_5,f_6,f_7,f_8,f_9,f_{10},f_{11},f_{12},x_{14},0\right)^T,\\ g_1 =&\left(0,\ 0,\ 0,\ 0,\ 0,\ 0,\ 0,\ 0,\ 0,\ 0,\ 0,\ 0,\ 0,\ 1\right)^T,\\ g_2 =&\left(0,\ 0,\ 0,\ 0,\ 0,\ 0,\ 0,\ 0,\ 0,\ \tfrac{d}{I_x},\ 0,\ 0,\ 0,\ 0\right)^T,\\ g_3 =&\left(0,\ 0,\ 0,\ 0,\ 0,\ 0,\ 0,\ 0,\ 0,\ 0,\ \tfrac{d}{I_y},\ 0,\ 0,\ 0\right)^T,\\ g_4 =&\left(0,\ 0,\ 0,\ 0,\ 0,\ 0,\ 0,\ 0,\ 0,\ 0,\ 0,\ \tfrac{1}{I_z}\ 0,\ 0\right)^T,\end{aligned}$$

$$
\begin{aligned}
h(x) &= \left(h_1, h_2, h_3, h_4\right)^T = \left(x_1, x_2, x_3, x_4\right)^T, \\
f_4 =& x_{11} \sum_{i_5=\sigma_5}^{\sigma_5+1} \sum_{i_6=\sigma_6}^{\sigma_6+1} \omega_5^{i_5}(x_5) \omega_6^{i_6}(x_6) f_{41}(i_5, i_6) \\
&+ x_{12} \sum_{i_5=\sigma_5}^{\sigma_5+1} \sum_{i_6=\sigma_6}^{\sigma_6+1} \omega_5^{i_5}(x_5) \omega_6^{i_6}(x_6) f_{42}(i_5, i_6), \\
f_5 =& x_{11} \sum_{i_6=\sigma_6}^{\sigma_6+1} \omega_6^{i_6}(x_6) f_{51}(i_6) - x_{12} \sum_{i_6=\sigma_6}^{\sigma_6+1} \omega_6^{i_6}(x_6) f_{52}(i_6), \\
f_6 =& x_{10} + x_{11} \sum_{i_5=\sigma_5}^{\sigma_5+1} \sum_{i_6=\sigma_6}^{\sigma_6+1} \omega_5^{i_5}(x_5) \omega_6^{i_6}(x_6) f_{61}(i_5, i_6) \\
&+ x_{12} \sum_{i_5=\sigma_5}^{\sigma_5+1} \sum_{i_6=\sigma_6}^{\sigma_6+1} \omega_5^{i_5}(x_5) \omega_6^{i_6}(x_6) f_{62}(i_5, i_6), \\
f_7 =& A_x/m + x_{13} \sum_{i_4=\sigma_4}^{\sigma_4+1} \sum_{i_5=\sigma_5}^{\sigma_5+1} \sum_{i_6=\sigma_6}^{\sigma_6+1} \omega_4^{i_4}(x_4) \omega_5^{i_5}(x_5) \\
&\times \omega_6^{i_6}(x_6) f_7(i_4, i_5, i_6), \\
f_8 =& A_y/m + x_{13} \sum_{i_4=\sigma_4}^{\sigma_4+1} \sum_{i_5=\sigma_5}^{\sigma_5+1} \sum_{i_6=\sigma_6}^{\sigma_6+1} \omega_4^{i_4}(x_4) \omega_5^{i_5}(x_5) \\
&\times \omega_6^{i_6}(x_6) f_8(i_4, i_5, i_6), \\
f_9 =& A_z/m + x_{13} \sum_{i_5=\sigma_5}^{\sigma_5+1} \sum_{i_6=\sigma_6}^{\sigma_6+1} \omega_5^{i_5}(x_5) \omega_6^{i_6}(x_6) f_9(i_5, i_6), \\
f_{10} =& \frac{I_y - I_z}{I_x} x_{11} x_{12} + \frac{A_p}{I_x}, \ f_{11} = \frac{I_z - I_x}{I_y} x_{12} x_{10} + \frac{A_q}{I_y}, \\
f_{12} =& \frac{I_x - I_y}{I_z} x_{10} x_{11} + \frac{A_r}{I_z}.
\end{aligned}
$$

In this paper, we construct the PML models with respect to trigonometric functions. Hence the state spaces of x_4, x_5 and x_6 are divided into some vertices. For example, the vertices $f_{41}(i_5, i_6)$ and $f_{42}(i_5, i_6)$ are given by substituting the vertices x_5 and x_6 for the nonlinear terms $\sin x_6 \sec x_5 (= \sin\phi \sec\theta)$ and $\cos x_6 \sec x_5 (= \cos\phi \sec\theta)$. Table I shows the vertices of PML model $f_{41}(i_5, i_6)$. In contrast, nonlinear terms of f_{10}, f_{11} and f_{12} are not transformed into the PML models. Since the nonlinear terms of f_{10}, f_{11} and f_{12} are multi-linear functions.

B. Stabilizing Control Using Dynamic Feedback Linearization Based on PML Model

The stabilizing conditions of PML system are represented by BMIs [23], therefore, it takes long computing time to obtain a stabilizing controller. In this paper, feedback linearization method is used for the controller design. Using the feedback linearization method as the controller designs, it is easy to design the continuous piecewise nonlinear controller for PML control system and the controller designs drastically reduce the time that it takes to find an optimal solution of the stabilizing condition by computer simulation. Therefore PML modeling and feedback linearizations could be a powerful combination for the analysis and synthesis of nonlinear control systems.

We define the output as $\eta = (\eta_1, \eta_2, \eta_3, \eta_4)^T = (x_1, x_2, x_3, x_4)^T$, the time derivative of η is calculated as

$$
\dot{\eta} = \begin{pmatrix} L_f h_1 \\ L_f h_2 \\ L_f h_3 \\ L_f h_4 \end{pmatrix} = \begin{pmatrix} \dot{x}_1 \\ \dot{x}_2 \\ \dot{x}_3 \\ \dot{x}_4 \end{pmatrix} = \begin{pmatrix} x_7 \\ x_8 \\ x_9 \\ f_4 \end{pmatrix}.
$$

The time derivative of η doesn't contain the control inputs (u_1, u_2, u_3, u_4). We calculate the time derivative of $\dot{\eta}$. We get

$$
\begin{aligned}
\ddot{\eta}_1 =& L_f^2 h_1 = f_7, \ \ddot{\eta}_2 = L_f^2 h_2 = f_8, \ \ddot{\eta}_3 = L_f^2 h_3 = f_9, \\
\ddot{\eta}_4 =& L_f^2 h_4 = \frac{\partial f_4}{\partial x_5} f_5 + \frac{\partial f_4}{\partial x_6} f_6 + \frac{\partial f_4}{\partial x_{11}} f_{11} + \frac{\partial f_4}{\partial x_{12}} f_{12} \\
&+ \frac{\partial f_4}{\partial x_{11}} d/I_y \mu_3 + \frac{\partial f_4}{\partial x_{12}} 1/I_z \mu_4,
\end{aligned}
$$

where

$$
\begin{aligned}
\frac{\partial f_4}{\partial x_5} =& x_{11} \sum_{i_6=\sigma_6}^{\sigma_6} \omega_6^{i_6}(x_6) \left(f_{41}(\sigma_5+1, i_6) - f_{41}(\sigma_5, i_6)\right)/\Delta_5 \\
&+ x_{12} \sum_{i_6=\sigma_6}^{\sigma_6} \omega_6^{i_6}(x_6) \left(f_{42}(\sigma_5+1, i_6) - f_{42}(\sigma_5, i_6)\right)/\Delta_5, \\
\frac{\partial f_4}{\partial x_6} =& x_{11} \sum_{i_5=\sigma_5}^{\sigma_5} \omega_5^{i_5}(x_5) \left(f_{41}(i_5, \sigma_6+1) - f_{41}(i_5, \sigma_6)\right)/\Delta_6 \\
&+ x_{12} \sum_{i_5=\sigma_5}^{\sigma_5} \omega_5^{i_5}(x_5) \left(f_{42}(i_5, \sigma_6+1) - f_{42}(i_5, \sigma_6)\right)/\Delta_6, \\
\frac{\partial f_4}{\partial x_{11}} =& \sum_{i_6=\sigma_6}^{\sigma_6+1} \omega_5^{i_5}(x_5) \omega_6^{i_6}(x_6) f_{41}(i_5, i_6), \\
\frac{\partial f_4}{\partial x_{12}} =& \sum_{i_6=\sigma_6}^{\sigma_6+1} \omega_5^{i_5}(x_5) \omega_6^{i_6}(x_6) f_{42}(i_5, i_6), \\
\Delta_5 =& d_5(\sigma_5+1) - d_5(\sigma_5), \ \Delta_6 = d_6(\sigma_6+1) - d_6(\sigma_6).
\end{aligned}
$$

We continue to calculate the time derivatives of $\ddot{\eta}_1$, $\ddot{\eta}_2$ and $\ddot{\eta}_3$. We get

$$
\begin{aligned}
\eta_1^{(3)} =& L_f^3 h_1 = \frac{\partial f_7}{\partial x_4} f_4 + \frac{\partial f_7}{\partial x_5} f_5 + \frac{\partial f_7}{\partial x_6} f_6 + \frac{\partial f_7}{\partial x_{13}} f_{13}, \\
\eta_2^{(3)} =& L_f^3 h_2 = \frac{\partial f_8}{\partial x_4} f_4 + \frac{\partial f_8}{\partial x_5} f_5 + \frac{\partial f_8}{\partial x_6} f_6 + \frac{\partial f_8}{\partial x_{13}} f_{13}, \\
\eta_3^{(3)} =& L_f^3 h_3 = \frac{\partial f_9}{\partial x_5} f_5 + \frac{\partial f_9}{\partial x_6} f_6 + \frac{\partial f_9}{\partial x_{13}} f_{13},
\end{aligned}
$$

where

$$
\begin{aligned}
\frac{\partial f_j}{\partial x_4} =& x_{13} \sum_{i_5=\sigma_5}^{\sigma_5+1} \sum_{i_6=\sigma_6}^{\sigma_6+1} \omega_5^{i_5}(x_5) \omega_6^{i_6}(x_6) \\
&\times \left(f_j(\sigma_4+1, i_5, i_6) - f_j(\sigma_4, i_5, i_6)\right)/\Delta_4, \\
\frac{\partial f_j}{\partial x_5} =& x_{13} \sum_{i_4=\sigma_4}^{\sigma_4+1} \sum_{i_6=\sigma_6}^{\sigma_6+1} \omega_4^{i_4}(x_4) \omega_6^{i_6}(x_6) \\
&\times \left(f_j(i_4, \sigma_5+1, i_6) - f_j(i_4, \sigma_5, i_6)\right)/\Delta_5,
\end{aligned}
$$

TABLE I
VERTICES OF PML MODEL $f_{41}(i_5, i_6)$

f_{41}	$x_6=-5\pi/12$	$x_6=-\delta_2$	$x_6=-\delta_2/2$	$x_6=0$	$x_6=\delta_2/2$	$x_6=\delta_2$	$x_6=5\pi/12$
$x_5=-5\pi/12$	−3.7321	−0.0607	−0.0303	0	0.0303	0.0607	3.7321
$x_5=-\delta_1$	−0.9660	−0.0157	−0.0079	0	0.0079	0.0157	0.9660
$x_5=-\delta_1/2$	−0.9660	−0.0157	−0.0079	0	0.0079	0.0157	0.9660
$x_5=0$	−0.9659	−0.0157	−0.0079	0	0.0079	0.0157	0.9659
$x_5=\delta_1/2$	−0.9660	−0.0157	−0.0079	0	0.0079	0.0157	0.9660
$x_5=\delta_1$	−0.9660	−0.0157	−0.0079	0	0.0079	0.0157	0.9660
$x_5=5\pi/12$	−3.7321	−0.0607	−0.0303	0	0.0303	0.0607	3.7321

$$\begin{aligned}
\frac{\partial f_j}{\partial x_6} =& x_{13} \sum_{i_4=\sigma_4}^{\sigma_4+1} \sum_{i_5=\sigma_5}^{\sigma_5+1} \omega_4^{i_4}(x_4)\omega_5^{i_5}(x_5) \\
& \times \left(f_j(i_4, i_5, \sigma_6) - f_j(i_4, i_5, \sigma_6+1)\right)/\Delta_6, \\
\frac{\partial f_j}{\partial x_{13}} =& \sum_{i_4=\sigma_4}^{\sigma_4+1} \sum_{i_5=\sigma_5}^{\sigma_5+1} \sum_{i_6=\sigma_6}^{\sigma_6+1} \\
& \times \omega_4^{i_4}(x_4)\omega_5^{i_5}(x_5)\omega_6^{i_6}(x_6) f_j(i_4, i_5, i_6), \\
\frac{\partial f_9}{\partial x_5} =& x_{13} \sum_{i_6=\sigma_6}^{\sigma_6+1} \omega_6^{i_6}(x_6)\left(f_9(\sigma_5+1, i_6) - f_9(\sigma_5, i_6)\right)/\Delta_5, \\
\frac{\partial f_9}{\partial x_6} =& x_{13} \sum_{i_5=\sigma_5}^{\sigma_5+1} \omega_5^{i_5}(x_5)\left(f_9(i_5, \sigma_6) - f_9(i_5, \sigma_6+1)\right)/\Delta_6, \\
\frac{\partial f_9}{\partial x_{13}} =& \sum_{i_5=\sigma_5}^{\sigma_5+1} \sum_{i_6=\sigma_6}^{\sigma_6+1} \omega_5^{i_5}(x_5)\omega_6^{i_6}(x_6) f_9(i_5, i_6),
\end{aligned}$$

$j = 7, 8$. Since $L_f^3 h_1$, $L_f^3 h_2$ and $L_f^3 h_3$ are independent of the controller u, we continue to calculate the time derivatives of $\eta_1^{(3)}$, $\eta_2^{(3)}$ and $\eta_3^{(3)}$.

$$\begin{aligned}
\eta_1^{(4)} =& L_f^4 h_1 + L_{g_1} L_f^3 h_1 \mu_1 + L_{g_2} L_f^3 h_1 \mu_2 + L_{g_3} L_f^3 h_1 \mu_3, \\
\eta_2^{(4)} =& L_f^4 h_2 + L_{g_1} L_f^3 h_2 \mu_1 + L_{g_2} L_f^3 h_2 \mu_2 + L_{g_3} L_f^3 h_2 \mu_3, \\
\eta_3^{(4)} =& L_f^4 h_3 + L_{g_1} L_f^3 h_3 \mu_1 + L_{g_2} L_f^3 h_3 \mu_2 + L_{g_3} L_f^3 h_3 \mu_3.
\end{aligned}$$

The details of the Lie derivatives are omitted due to lack of space. The controller of (20) is designed as

$$\mu = \alpha(x) + \beta(x)v$$

where $\alpha(x) = -A_{qr}^{-1}(x)B_{qr}(x)$, $\beta(x) = A_{qr}^{-1}(x)$,

$$A_{qr}(x) = \begin{pmatrix} L_{g_1} L_f^3 h_1 & L_{g_2} L_f^3 h_1 & L_{g_3} L_f^3 h_1 & 0 \\ L_{g_1} L_f^3 h_2 & L_{g_2} L_f^3 h_2 & L_{g_3} L_f^3 h_2 & 0 \\ L_{g_1} L_f^3 h_3 & L_{g_2} L_f^3 h_3 & L_{g_3} L_f^3 h_3 & 0 \\ 0 & 0 & L_{g_3} L_f h_4 & L_{g_4} L_f h_4 \end{pmatrix},$$
$$B_{qr}(x) = \left(L_f^4 h_1,\ L_f^4 h_2,\ L_f^4 h_3,\ L_f^2 h_4\right)^T,$$

$v = -Fz$ is the linear controller of the linear system (21).

$$\begin{cases} \dot{z} =& Az + Bu, \\ y =& Cz, \end{cases} \tag{21}$$

where

$$\begin{aligned}
& z = \left(z_1,\ z_2,\ z_3,\ z_4\right)^T \in \Re^{14}, \\
& z_1 = \left(h_1,\ L_f h_1,\ L_f^2 h_1,\ L_f^3 h_1\right)^T, \\
& z_2 = \left(h_2,\ L_f h_2,\ L_f^2 h_2,\ L_f^3 h_2,\right)^T, \\
& z_3 = \left(h_3,\ L_f h_3,\ L_f^2 h_3,\ L_f^3 h_3\right)^T, \\
& z_4 = \left(h_4,\ L_f h_4\right)^T, \\
& A = \text{blockdiag}(A_1, A_2, A_3, A_4), \\
& B = \begin{pmatrix} B_1^T & B_2^T & B_3^T & B_4^T \end{pmatrix}^T, \\
& C = \text{blockdiag}(C_1, C_2, C_3, C_4), \\
& A_1 = \begin{pmatrix} 0 & 1 & 0 & 0 \\ 0 & 0 & 1 & 0 \\ 0 & 0 & 0 & 1 \\ 0 & 0 & 0 & 0 \end{pmatrix}, A_1 = A_2 = A_3, A_4 = \begin{pmatrix} 0 & 1 \\ 0 & 0 \end{pmatrix}, \\
& B_1 = \begin{pmatrix} 0 & 0 & 0 & 0 \\ 0 & 0 & 0 & 0 \\ 0 & 0 & 0 & 0 \\ 1 & 0 & 0 & 0 \end{pmatrix}, B_2 = \begin{pmatrix} 0 & 0 & 0 & 0 \\ 0 & 0 & 0 & 0 \\ 0 & 0 & 0 & 0 \\ 0 & 1 & 0 & 0 \end{pmatrix}, \\
& B_3 = \begin{pmatrix} 0 & 0 & 0 & 0 \\ 0 & 0 & 0 & 0 \\ 0 & 0 & 0 & 0 \\ 0 & 0 & 1 & 0 \end{pmatrix}, B_4 = \begin{pmatrix} 0 & 0 & 0 & 0 \\ 0 & 0 & 0 & 1 \end{pmatrix}, \\
& C_1 = \begin{pmatrix} 1 & 0 & 0 & 0 \end{pmatrix}, C_1 = C_2 = C_3, C_4 = \begin{pmatrix} 1 & 0 \end{pmatrix}.
\end{aligned}$$

In this case, the state space of the quadrotor helicopter robot model is divided into $13 \times 7 \times 7$ vertices. Therefore the system has $12 \times 6 \times 6$ local PML models. Note that all the linearized systems of these PML models are the same as the linear system (21).

The dynamic feedback linearizing controller of the PML system (20) is designed as

$$\begin{cases} \ddot{u}_1 =& \mu_1, \\ u_i =& \mu_i, \quad i = 2, 3, 4 \end{cases} \tag{22}$$

The stabilizing linear controller $v = -Fz$ of the linearized system (21) is designed so that the transfer function $C(sI - A)^{-1}B$ is Hurwitz.

Note that the dynamic controller (22) based on PML model is simpler than the conventional one. Since the nonlinear terms of controller (22) contain not the original nonlinear terms (e.g., $\sin\phi$, $\cos\phi$, $\sec\theta$) but the piecewise approximation models.

C. Trajectory Tracking Controller Based on PML System

We propose a trajectory tracking control to the quadrotor helicopter robot model (12). Consider the following reference signal model

$$\begin{cases} \dot{x}_r = f_r, \\ \eta_r = h_r. \end{cases}$$

The controller is designed to make the error signal $e = (e_1, e_2, e_3, e_4)^T = \eta - \eta_r \to 0$ as $t \to \infty$. The time derivative of e is obtained as

$$\dot{e} = \dot{\eta} - \dot{\eta}_r = \begin{pmatrix} L_f h_1 \\ L_f h_2 \\ L_f h_3 \\ L_f h_4 \end{pmatrix} - \begin{pmatrix} L_{f_r} h_{r1} \\ L_{f_r} h_{r2} \\ L_{f_r} h_{r1} \\ L_{f_r} h_{r2} \end{pmatrix}.$$

Furthermore the time derivative of $\dot{e}$ is calculated as

$$\ddot{e} = \begin{pmatrix} L_f^2 h_1 \\ L_f^2 h_2 \\ L_f^2 h_3 \\ L_f^2 h_4 + L_{g_3} L_f h_4 u_3 + L_{g_4} L_f h_4 u_4 \end{pmatrix} - \begin{pmatrix} L_{f_r}^2 h_{r1} \\ L_{f_r}^2 h_{r2} \\ L_{f_r}^2 h_{r3} \\ L_{f_r}^2 h_{r4} \end{pmatrix}.$$

Since the controller u doesn't appear in the equations $\ddot{e}_1$, $\ddot{e}_2$ and $\ddot{e}_3$ we calculate the time derivative of $\ddot{e}_i$ $(i = 1, 2, 3)$.

$$\begin{pmatrix} e_1^{(3)} \\ e_2^{(3)} \\ e_3^{(3)} \end{pmatrix} = \begin{pmatrix} L_f^3 h_1 \\ L_f^3 h_2 \\ L_f^3 h_3 \end{pmatrix} - \begin{pmatrix} L_{f_r}^3 h_{r1} \\ L_{f_r}^3 h_{r2} \\ L_{f_r}^3 h_{r3} \end{pmatrix}$$

We continue to calculate the time derivatives of $e_i^{(3)}$ $(i = 1, 2, 3)$.

$$\begin{aligned} \begin{pmatrix} e_1^{(4)} \\ e_2^{(4)} \\ e_3^{(4)} \end{pmatrix} &= \begin{pmatrix} L_f^4 h_1 \\ L_f^4 h_2 \\ L_f^4 h_3 \end{pmatrix} - \begin{pmatrix} L_{f_r}^4 h_{r1} \\ L_{f_r}^4 h_{r2} \\ L_{f_r}^4 h_{r3} \end{pmatrix} \\ &+ \begin{pmatrix} L_{g_1} L_f^3 h_1 \mu_1 + L_{g_2} L_f^3 h_1 \mu_2 + L_{g_1} L_f^3 h_1 \mu_3 \\ L_{g_1} L_f^3 h_2 \mu_1 + L_{g_2} L_f^3 h_2 \mu_2 + L_{g_1} L_f^3 h_2 \mu_3 \\ L_{g_1} L_f^3 h_3 \mu_1 + L_{g_2} L_f^3 h_3 \mu_2 + L_{g_1} L_f^3 h_3 \mu_3 \end{pmatrix} \end{aligned}$$

The tracking controller is designed as

$$\begin{cases} \ddot{u}_1 = \mu_1, \\ u_i = \mu_i, \quad i = 2, 3, 4. \end{cases} \tag{23}$$

The linearized system (21) and controller $v = -Fz$ are obtained in the same manners as the previous subsection. The coordinate transformation vector is $z = (e_1, \dot{e}_1, \ddot{e}_1, e_1^{(3)}, e_2, \dot{e}_2, \ddot{e}_2, e_2^{(3)}, e_3, \dot{e}_3, \ddot{e}_3, e_3^{(3)}, e_4, \dot{e}_4)^T$.

Note that the dynamic controller (23) based on PML model is simpler than the conventional one on the same reason of the previous subsection.

VI. Simulation results

We apply the trajectory tracking control to the tricycle robot model (7) and the quadrotor helicopter model (12). Although the controller is simpler than the conventional I/O feedback linearization controller, the tracking performance based on PML model is the same as the conventional one. In addition, the controller is capable to use a nonlinear system with chaotic behavior as the reference model.

A. Tricycle Model

In the following simulations, the tricycle length L is 1.0 [m] and the angle constrain M is $\pi/3$ [rad.].

1) Ellipse-shaped Reference Signal: Consider an ellipse model as the reference trajectory.

$$\begin{pmatrix} x_{r_1} \\ x_{r_2} \end{pmatrix} = \begin{pmatrix} R_1 \cos\theta + x_{r_1}(0) \\ R_2 \sin\theta + x_{r_2}(0) \end{pmatrix},$$

where R_1 and R_2 are the semiminor axes and $(x_{r_1}(0), x_{r_2}(0))$ is the center of the ellipse. Fig. 4 shows the simulation result. The dotted line is the reference signal and the solid line is the tricycle tracking trajectory. The semiminor parameters R_1 and R_2 are 10 and 25. The initial positions are set at $(x(0), y(0)) = (5, 0)$ and $(x_r(0), y_r(0)) = (10, 0)$. Fig. 5 shows the control inputs u_1 and ν_1 of the tricycle. Fig. 6 shows the error signals of the tricycle position (x, y).

2) Trajectory Tracking Control Using Some Ellipse-shaped Reference Signals: Arbitrary tracking trajectory control can be realized using the ellipse-shaped tracking trajectory method. The controller design procedure is as follows:

1) Assign passing points $(p_x(i), p_y(i))$, $i = 1, \ldots, n$.
   We consider the passing points: $(0, 0)$, $(10, 20)$, $(26, 30)$, $(18, 50)$ and $(2, 70)$
2) Construct some ellipses trajectories to connect the passing points smoothly.
   From $(0, 0)$ to $(10, 20)$, the trajectory 1:
   $$\begin{pmatrix} x_{r_1} \\ x_{r_2} \end{pmatrix} = \begin{pmatrix} 10\cos\theta_r + 10 \\ 20\sin\theta_r \end{pmatrix}, \tag{24}$$
   where $\pi/2 \le \theta_r \le \pi$.
   From $(10, 20)$ to $(26, 30)$, the trajectory 2:
   $$\begin{pmatrix} x_{r_1} \\ x_{r_2} \end{pmatrix} = \begin{pmatrix} 16\cos\theta_r + 10 \\ 10\sin\theta_r + 30 \end{pmatrix}, \tag{25}$$
   where $-\pi/2 \le \theta_r \le 0$.
   From $(26, 30)$ to $(18, 50)$, the trajectory 3:
   $$\begin{pmatrix} x_{r_1} \\ x_{r_2} \end{pmatrix} = \begin{pmatrix} 8\cos\theta_r + 18 \\ 20\sin\theta_r + 30 \end{pmatrix}, \tag{26}$$
   where $0 \le \theta_r \le \pi/2$.
   From $(18, 50)$ to $(2, 70)$, the trajectory 4:
   $$\begin{pmatrix} x_{r_1} \\ x_{r_2} \end{pmatrix} = \begin{pmatrix} 16\cos\theta_r + 18 \\ 10\sin\theta_r + 60 \end{pmatrix}, \tag{27}$$
   where $-\pi/2 \le \theta_r \le -\pi/2$.
3) Design the controllers (19) for the ellipse tracking trajectories (24)-(27).

We show a tracking trajectory control example for the tricycle robot system. Fig. 7 shows the reference signals (24)-(27) and the tricycle tracking trajectory. The dotted line is the reference signal and the solid line is the tricycle tracking trajectory. Fig. 8 shows the control inputs u_1 and ν_1 of the tricycle. Fig. 9 shows the error signals with respect to the tricycle position (x, y).

B. Quadrotor Helicopter Model

1) Spiral descent reference trajectory: We consider two tracking trajectories as the reference signals. Although the controllers are simpler than the conventional I/O feedback linearization controllers, the tracking performance based on PML model is the same as the conventional one [16].

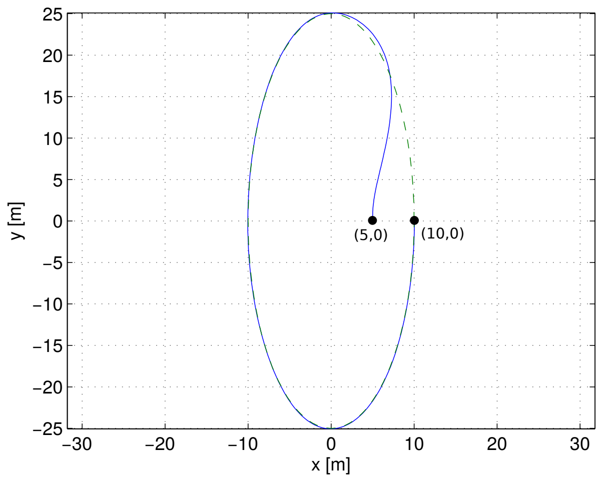

Fig. 4. Ellipse-shaped reference signal and the tricycle tracking trajectory

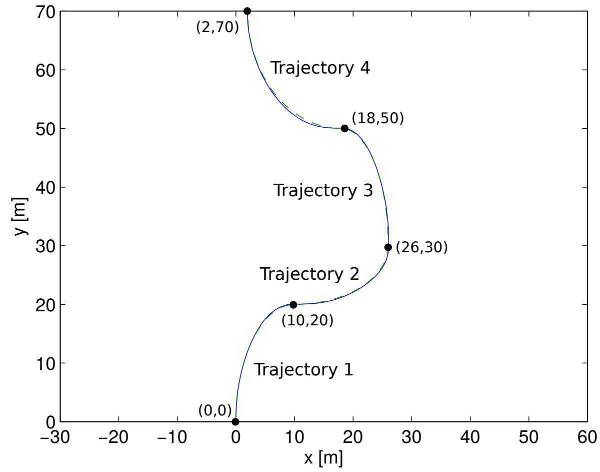

Fig. 7. Reference signals (24)-(27) and the tricycle tracking trajectory

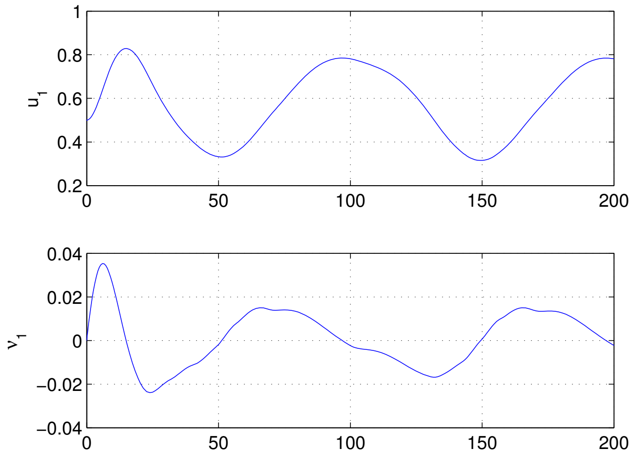

Fig. 5. Control inputs u_1 and ν_1 of the tricycle

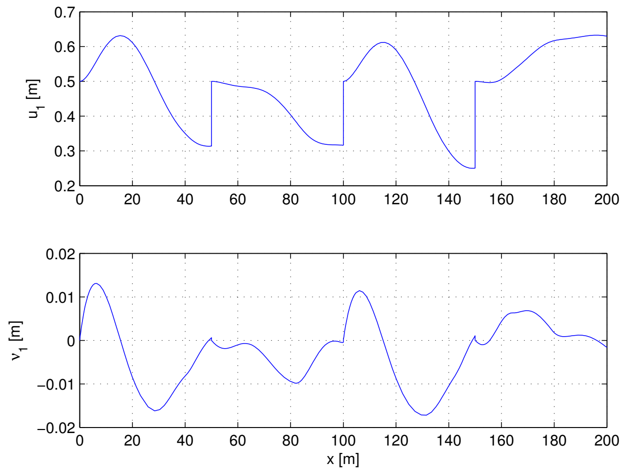

Fig. 8. Control inputs u_1 and ν_1 of the tricycle

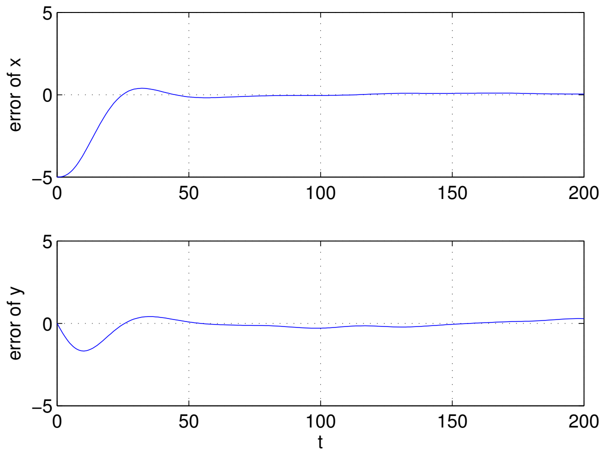

Fig. 6. Error signals of the tricycle position (x, y)

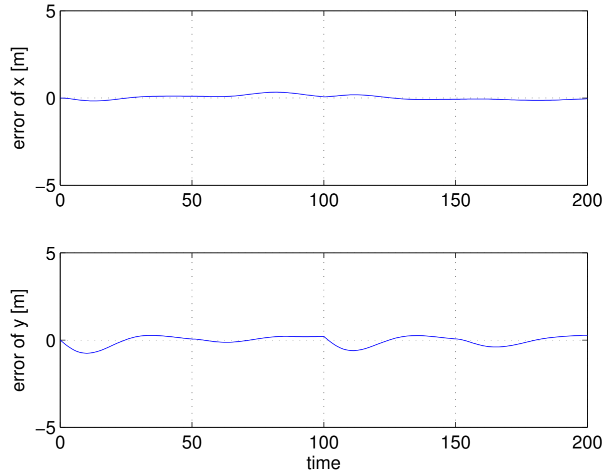

Fig. 9. Error signals of the tricycle position (x, y)

Consider a spiral-shaped reference trajectory [16] as the reference model.

$$\begin{cases} x_{d_1} = \frac{1}{2}\cos\frac{t}{2},\ x_{d_2} = \frac{1}{2}\sin\frac{t}{2}, \\ x_{d_3} = -1 - \frac{t}{10},\ x_{d_4} = \frac{\pi}{3}. \end{cases} \tag{28}$$

The feedback gain is calculated as

$$F = \begin{pmatrix} F_1 & 0 & 0 & 0 \\ 0 & F_1 & 0 & 0 \\ 0 & 0 & F_1 & 0 \\ 0 & 0 & 0 & F_2 \end{pmatrix},$$

$$F_1 = (1.000, 3.078, 4.236, 3.078),$$
$$F_2 = (1.000, 1.732).$$

The helicopter is initially in hover flight and the initial positions are set at $(x_1, x_2, x_3, x_4) = (0, 0, 0, 0)$ and $(x_{r_1}, x_{r_2}, x_{r_3}, x_{r_4}) = (1/2, 0, 1, \pi/3)$. In this simulation, the parameters are given by $m = 0.7$, $I_x = I_y = I_z = 1.242$, $d = 0.3$ and $g = 9.81$. Fig. 10 shows the trajectory signals. The solid line is the state response (x_1, x_2, x_3) of the helicopter and the dotted line is the reference signal (28).

2) Spiral ascending reference trajectory: Consider a spiral-shaped reference trajectory [16] as the reference model.

$$\begin{cases} x_{d_1} = \frac{1}{2}\cos\frac{t}{2},\ x_{d_2} = \frac{1}{2}\sin\frac{t}{2}, \\ x_{d_3} = 1 + \frac{t}{10},\ x_{d_4} = \frac{\pi}{3}. \end{cases} \tag{29}$$

The feedback gain is the same as the previous example. The helicopter is initially in hover flight and the initial positions are set at $(x_1, x_2, x_3, x_4) = (0, 0, 0, 0)$ and $(x_{r_1}, x_{r_2}, x_{r_3}, x_{r_4}) = (1/2, 0, 1, \pi/3)$. In this simulation, the parameters are given by $m = 0.7$, $I_x = I_y = I_z = 1.242$, $d = 0.3$ and $g = 9.81$. Fig. 11 shows the trajectory signals. The solid line is the state response (x_1, x_2, x_3) of the helicopter and the dotted line is the reference signal (29).

These results confirm the feasibility of the tracking control performance. Although the PML model (20) and the controller (19) are simpler than the conventional dynamic feedback linearization controller and model [16], the control performance based on PML model is the same as the conventional one [16].

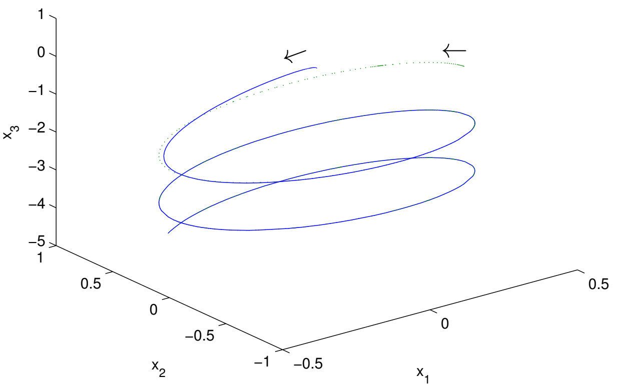

Fig. 10. Decent reference trajectories

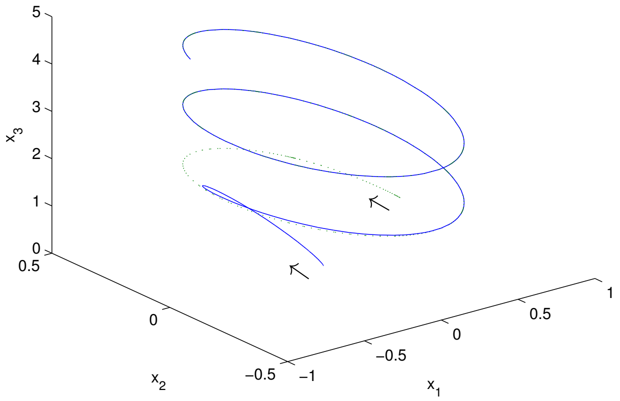

Fig. 11. Ascending reference trajectories

3) Trajectory Tracking Control Using Some Ellipse-shaped Reference Signals: Arbitrary tracking trajectory control can be realized using the ellipse-shaped tracking trajectory method. The controller design procedure is as follows:

1) Assign passing points $(p_x(i), p_y(i), p_z(i))$, $i = 1, \ldots, n$. We consider the passing points: $(0, 0, 0)$, $(5, 0, 2)$, $(4, 0, 3)$ and $(0, 0, 0)$.
2) Construct these trajectories to connect the passing points smoothly.
From $(0, 0, 0)$ to $(5, 0, 2)$, the trajectory 1 is
$$\begin{pmatrix} x_{r_1} \\ x_{r_2} \\ x_{r_3} \end{pmatrix} = \begin{pmatrix} 5\sin\theta_r\cos\varphi_r \\ \sin\theta_r\sin\varphi_r \\ 2\cos\theta_r + 2 \end{pmatrix}, \tag{30}$$
where $\pi/2 \le \theta_r \le \pi$ and $\varphi = 0$.
From $(5, 0, 2)$ to $(4, 0, 3)$, the trajectory 2 is
$$\begin{pmatrix} x_{r_1} \\ x_{r_2} \\ x_{r_3} \end{pmatrix} = \begin{pmatrix} \frac{1}{2}\cos t + \frac{9}{2} \\ \frac{1}{2}\sin t \\ 2 + \frac{t}{5\pi} \end{pmatrix}. \tag{31}$$
From $(4, 0, 3)$ to $(0, 0, 0)$, the trajectory 3 is
$$\begin{pmatrix} x_{r_1} \\ x_{r_2} \\ x_{r_3} \end{pmatrix} = \begin{pmatrix} 4\sin\theta_r\cos\varphi_r + 4 \\ \sin\theta_r\sin\varphi_r \\ 3\cos\theta_r \end{pmatrix}, \tag{32}$$
where $-\pi/2 \le \theta_r \le 0$ and $\varphi_r = 0$.
3) Design the controllers (23) for the ellipse tracking trajectories (30)-(32).

We show the simulation result for the quadrotor helicopter system. Fig. 12 shows the reference signals (30)-(32) and the quadrotor helicopter tracking trajectory. The dotted line is the reference signal and the solid line is the tricycle tracking trajectory.

VII. Conclusions

We have proposed the trajectory tracking controller designs of a tricycle robot and a quadrotor as non-holonomic systems based on PML models. The approximated model are fully parametric. I/O dynamic feedback linearization is applied to stabilize PML control system. PML modeling with feedback linearization is a very powerful tool for analyzing and synthesizing nonlinear control systems. We also have designed the tracking controllers to the tricycle robot and the quadrotor. Although the controllers are simpler than the conventional I/O feedback linearization controller, the

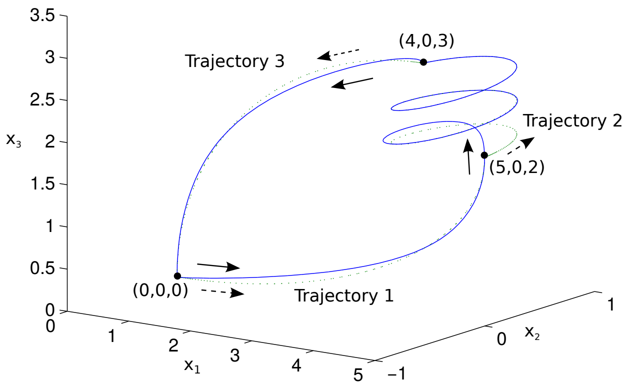

Fig. 12. Reference signals (30)-(32) and the tracking trajectory of the quadrotor helicopter system

tracking performance based on PML model is the same as the conventional one. The examples have been shown to confirm the feasibility of our proposals by computer simulations.

References

[1] R. W. Brockett, *Asymptotic stability and feedback stabilization, Differential Geometric Control Theory*. Boston: Birkhäuser, 1983, pp. 181–191.

[2] B. d'Andréa-Novel, G. Bastin, and G. Campion, "Modeling and control of non holonomic wheeled mobile robots," in *the 1991 IEEE International Conference on Robotics and Automation*, 1991, pp. 1130–1135.

[3] K. Kimura, S. Nozawa, Y. Kakiuchi, K. Okada, and M. Inaba, "Tricycle manipulation strategy for humanoid robot based on active and passive manipulators control," pp. 5797–5804.

[4] F. Kallasi, D. L. Rizzni, F. Oleari, M. Magnani, and S. Caselli, "A novel calibration method for industrial agvs," *Robotics and Autonomouse Systems*, vol. 94, pp. 75–88, 2017.

[5] R. Fierro and F. L. Lewis, "Control of a nonholonomic mobile robot: backstepping kinematics into dynamics," in *the 34th Conference on Decision and Control*, 1995, pp. 3805–3810.

[6] T.-C. Lee, K.-T. Song, C.-H. Lee, and C.-C. Teng, "Tracking control of unicycle-modeled mobile robots using a saturation feedback controller," *IEEE Transactions on Control Systems Technology*, vol. 9, no. 2, pp. 305–318, 2001.

[7] J. Guldner and V. I. Utkin, "Stabilization of non-holonomic mobile robots using lyapunov functions for navigation and sliding mode control," in *the 33rd Conference on Decision and Control*, 1994, pp. 2967–2972.

[8] J. Yang and J. Kim, "Sliding mode control for trajectory tracking of nonholonomic wheeled mobile robots," *IEEE Transactions on Robotics and Automation*, pp. 578–587, 1999.

[9] B. d'Andréa-Novel, G. Bastin, and G. Campion, "Dynamic feedback linearization of nonholonomic wheeled mobile robot," in *the 1992 IEEE International Conference on Robotics and Automation*, 1992, pp. 2527–2531.

[10] G. Oriolo, A. D. Luca, and M. Vendittelli, "WMR control via dynamic feedback linearization: Design, implementation, and experimental validation," *IEEE Transaction on Control System Technology*, vol. 10, no. 6, pp. 835–852, 2002.

[11] E. Yang, D. Gu, T. Mita, and H. Hu, "Nonlinear tracking control of a car-like mobile robot via dynamic feedback linearization," in *University of Bath, UK*, no. ID-218, 2004.

[12] A. D. Luca, G. Oriolo, and M. Vendittelli, "Stabilization of the unicycle via dynamic feedback linearization," in *the 6th IFAC Symposium on Robot Control*, 2000.

[13] R. Xu and U. Özgüner, "Sliding Mode Control of a Quadrotor Heilicopter," in *Proceedings of the 45th IEEE Conference on Decision & Control*, 2006, pp. 4957–4962.

[14] A. Gessow and G. Myers, *Aerodynamics of the helicopter*, third edition ed. New York: Frederick Ungar Publishing Co., 1967.

[15] E. Altug, J. P. Ostrowski, and R. Mahony, "Control of a Quadrotor Helicopter Using Visual Feedback," in *Proceedings of the 2002 IEEE International Conference on Robotics & Automation*, 2002, pp. 72–77.

[16] V. Mistler, A. Benallegue, and N. M'Sirdi, "Exact linearization and noninteracting control of a 4 rotors helicopter via dynamic feedback," in *IEEE International Workshop on Robot and Human Interactive Communication*, 2001, pp. 586–593.

[17] M. Bouchoucha, S. Seghour, and M. Tadjine, "Classical and Second Order Sliding Mode Control Solution to an Attitude Stabilization of a Four Rotors Helicopter : from Theory to Experiment," in *Proceedings of the 2011 IEEE International Conference on Mechatronics*, 2011, pp. 162–169.

[18] A. Benallegue, A. Mokhtari, and L. Fridman, "Feedback Linearization and High Order Sliding Mode Observer For A Quadrotor UAV," in *Proceedings of the 2006 International Workshop on Variable Structure Systems*, 2006, pp. 365–372.

[19] L. Derafa, L. Fridman, A. Benallegue, and A. Ouldali, "Super Twisting Control Algorithm for the Four Rotors Helicopter Attitude Tracking Problem," in *11th International Workshop on Variable Structure Systems*, 2010, pp. 62–67.

[20] C. Zhang, X. Zhou, H. Zhao, A. Dai, and H. Zhou, "Three-dimensional fuzzy control of mini quadrotor uav trajectory tracking under impact of wind disturbance," in *Proceedings of the 2016 International Conference on Advanced Mechatronic Systems*, 2016, pp. 372–377.

[21] J. Hwangbo, I. Sa, R. Siegwart, and M. Hutter, "Control of a quadrotor with reinforcement learning," *IEEE Robotics and Automation Letters*, vol. 2, no. 4, pp. 2096–2103, 2017.

[22] M. Sugeno, "On stability of fuzzy systems expressed by fuzzy rules with singleton consequents," *IEEE Trans. Fuzzy Syst.*, vol. 7, no. 2, pp. 201–224, 1999.

[23] K.-C. Goh, M. G. Safonov, and G. P. Papavassilopoulos, "A global optimization approach for the BMI problem," in *Proc. the 33rd IEEE CDC*, 1994, pp. 2009–2014.

[24] T. Taniguchi and M. Sugeno, "Piecewise bilinear system control based on full-state feedback linearization," in *SCIS & ISIS 2010*, 2010, pp. 1591–1596.

[25] ——, "Stabilization of nonlinear systems with piecewise bilinear models derived from fuzzy if-then rules with singletons," in *FUZZ-IEEE 2010*, 2010, pp. 2926–2931.

[26] ——, "Design of LUT-controllers for nonlinear systems with PB models based on I/O linearization," in *FUZZ-IEEE 2012*, 2012, pp. 997–1022.

[27] ——, "Trajectory tracking controller design for a tricycle robot using piecewise multi-linear models," in *Lecture Notes in Engineering and Computer Science: Proceedings of The International MultiConference of Engineers and Computer Scientists 2017,15-17 March, 2017, Hong Kong*, 2017, pp. 188–193.

[28] T. Taniguchi, L. Eciolaza, and M. Sugeno, "Look-Up-Table controller design for nonlinear servo systems with piecewise bilinear models," in *FUZZ-IEEE 2013*, 2013.

[29] ——, "Quadrotor control using dynamic feedback linearization based on piecewise bilinear models," in *2014 IEEE Symposium Series on Computational Intelligence*, 2014.

Tadanari Taniguchi receive the Doctor of Engineering degree from the University of Electro-Communications, Tokyo, Japan, in 2001. He was born in Toyama, Japan, in 1971. He graduated from the University of Electro-Communications. His research interests include intelligent control and nonlinear control. From 2001 to 2005, he was a research scientist at Brain Science Institute, RIKEN, Japan. Then he has served Tokai University, Kanagawa, Japan since 2005. He was a Visiting Scientist with Universite de Valenciennes, France, in 2015. He is currently an Associate Professor of Tokai University. He received a Best Paper Award of The 2017 IAENG International Conference on Control and Automation.

Michio Sugeno was born in Yokohama, Japan, in 1940. He graduated from the Department of Physics, The University of Tokyo, Tokyo, Japan. He then worked with Mitsubishi Atomic Power Industry. Then, he served the Tokyo Institute of Technology as a Research Associate, an Associate Professor, and a Professor from 1965 to 2000. After retiring from the Tokyo Institute of Technology, he was a Laboratory Head at the Brain Science Institute, RIKEN, from 2000 to 2005, and then, as a Distinguished Visiting Professor with Doshisha University from 2005 to 2010. He is currently an Emeritus Professor with the Tokyo Institute of Technology, Tokyo. Dr. Sugeno was the President of the Japan Society for Fuzzy Theory and Systems from 1991 to 1993, and also the President of the International Fuzzy Systems Association from 1997 to 1999. He is the first recipient of the IEEE Pioneer Award in Fuzzy Systems with Zadeh in 2000. He also received the 2010 IEEE Frank Rosenblatt Award and Kampt de Ferit Award in 2012.